FI SEVIER

Contents lists available at ScienceDirect

Optics Communications

journal homepage: www.elsevier.com/locate/optcom



Two-photon flow cytometry with laser scanning two-dimensional airy beams



Aurelio Paez ^{a,1}, Emma M. Sundin ^a, Gilberto Navarro ^b, Xiujun Li ^c, Thomas Boland ^a, Chunqiang Li ^{b,*}

- ^a Department of Metallurgical, Materials and Biomedical Engineering, The University of Texas at El Paso, 500 W University Avenue, El Paso, TX 79968, USA
- b Department of Physics, The University of Texas at El Paso, 500 W University Avenue, El Paso, TX 79968, USA
- Department of Chemistry and Biochemistry, The University of Texas at El Paso, 500 W University Avenue, El Paso, TX 79968, USA

ARTICLE INFO

Keywords: Airy beams Non-diffracting beams Two-photon excitation Fluorescence

ABSTRACT

Flow cytometry is an essential technique in biomedical discovery for cell counting, cell sorting, and biomarker detection. *In vivo* flow cytometers based on one-photon or two-photon excited fluorescence have been developed for over a decade. One drawback of the laser beam scanning two-photon flow cytometer is that the two-photon excitation volume is limited to the focal spot due to the short Rayleigh range of focused Gaussian beams. Hence, the sampling volume is much smaller than in one-photon flow cytometers, making it challenging to count or detect rare circulating cells *in vivo*. Non-diffracting light waves like Bessel beams and Airy beams have narrow intensity profiles with an effective spot size as small as several wavelengths, making them comparable to Gaussian beams. More significantly, the theoretical depth of field (propagation distance without diffraction) can be infinite, making them an ideal solution as a light source for scanning beam flow cytometry. The trade-off of using Airy beams rather than Gaussian beams is side lobes Airy beams have, which contribute to background noise. Two-photon excitation can reduce this noise, as the excitation efficiency is proportional to intensity squared. Therefore, we developed a two-photon flow cytometer using 2D Airy beams to form a light-sheet that intersects the blood vessel a microfluidic channel, which was used to model a blood vessel. The setup can successfully detect and count flowing fluorescent microspheres in a microchannel.

1. Introduction

Flow cytometry is commonly used in classifying cell types in biomedical research and clinical diagnosis [1]. In the last decade, in vivo flow cytometry has emerged as an essential tool to count circulating cells and detect biomarkers with broad applications in quantifying circulating tumor cells, immune cells, and red blood cells [2-4]. Threedimensional reconstructed imaging of cells has also been demonstrated in vitro using continuous microscopic flow cytometry techniques [5,6]. These quantitative studies provide information on tumor cell metastasis [7-16], tumor-secreted molecules [17], immune response [18], malaria diagnosis [19], sickled red blood cells [20], and circulating blood clots [21]. Most in vivo flow cytometers use laser light for excitation to detect the subsequent fluorescence, acoustic signals, or scattering after the light is absorbed/scattered by molecules within cells. One big challenge for in vivo flow cytometry is the limited detection depth due to tissue scattering of light, which makes it only suitable for detecting superficial vessels in mouse ears, retinas, or tails [15,16] unless techniques are used to optically clear the tissue [22,23]. Multiphoton excitation using

infrared lasers has the advantage of deeper penetration depth over onephoton excitation using visible lasers due to less tissue scattering in the near IR wavelength region and has achieved 1.4 mm penetration depth in fluorescence microscopic imaging of mouse brain tissue [24]. Therefore, integrating two-photon fluorescence into *in vivo* flow cytometry has been an ongoing research effort [9,25–27].

However, this improvement in penetration depth from two-photon excitation comes at the cost of reduced sampling volume. Typically, the laser beam is focused by a cylindrical lens to form a light-sheet to provide good cross-sectioning of blood vessels under one-photon excitation [2]. Two-photon excitation is a nonlinear process, which can only achieve efficient excitation within the focal volume of a focused Gaussian beam. The laser beam is scanned to cross-section the vessel. The focusing depth (Rayleigh range) of Gaussian beams (<1 μm) is usually much smaller than the diameter of blood vessels (10-100 μm). Therefore, the sampling volume of a conventional two-photon flow cytometer is much smaller than that of a one-photon flow cytometer. A larger light-sheet permits the cross-sectioning of larger-diameter vessels allowing for the sampling of larger volumes of blood per unit time. These larger light-sheets with efficient excitation can therefore make *in*

^{*} Corresponding author.

E-mail addresses: aurelio.paez@nasa.gov (A. Paez), emsundin@miners.utep.edu (E.M. Sundin), gnavarro4@miners.utep.edu (G. Navarro), xli4@utep.edu (X. Li), tboland@utep.edu (T. Boland), cli@utep.edu (C. Li).

¹ Current affiliation: NASA Marshall Space Flight Center, Martin Road SW, Huntsville, AL 35808, USA.

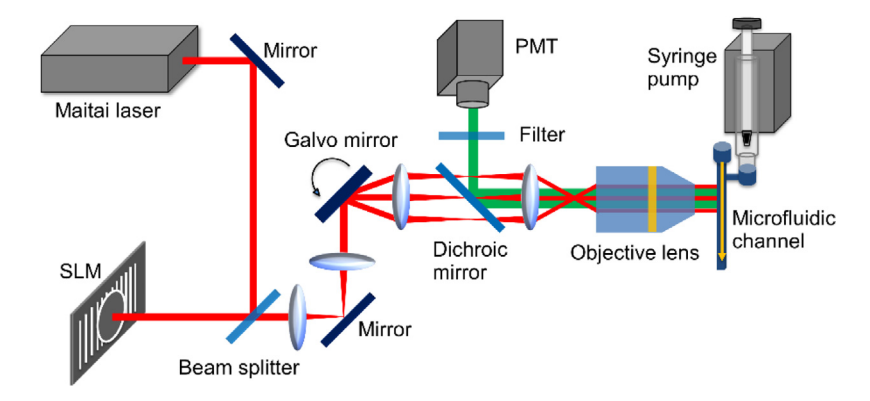


Fig. 1. Experimental setup of a laser scanning two-photon flow cytometer with Airy beams. PMT: photomultiplier tube, SLM: spatial light modulator.

vivo flow cytometry more practical for use as a clinical diagnostic tool by increasing the sampling speed. This is particularly true for detecting rare cells or particles, where large volumes of blood may need to be sampled [28].

Light-sheet microscopy, also called selective plane illumination microscopy, was developed more than two decades ago [29]. Two-photon excitation has been successfully incorporated into laser scanning lightsheet microscopy with a significantly improved penetration depth [30], increasing the possibility of high-speed deep tissue imaging. Typically, the laser beam used is a fundamental Gaussian beam, and the beam diverges quickly while moving away from its focal spot. The light sheet formed from this scanned Gaussian beam is non-uniform due to this rapid divergence. The center of the light sheet has a thinner depth since it is made of focused Gaussian beam spots, while the two ends of the light sheet are thicker due to the divergence of the Gaussian beam. This anisotropic light distribution degrades image quality since the excitation efficiencies from each end are much lower than that from the center. Bessel beams are Bessel-function solutions for scalar wave equations with non-diffracting characteristics [31-33]. These beams can have narrow intensity profiles with an effective spot size (FWHM) as small as several wavelengths, making them comparable to Gaussian beams. More significantly, the theoretical depth of field (propagation distance without diffraction) can be infinite, making it an ideal solution as a light source for scanning beam light-sheet microscopy [34–36]. The trade-off of using Bessel beams rather than Gaussian beams is would be the increase in background noise due to the concentric rings that Bessel beams have. In order to achieve good axial resolution, a structured illumination approach is typically applied to remove signals generated by the concentric side rings [34]. Two-photon excitation can reduce this noise as the excitation efficiency is proportional to intensity squared [37-40]. The use of Bessel beams to generate light-sheets for twophoton flow cytometry has been developed for counting fluorescent particles in microfluidic channels [41].

Bessel beams belong to a family of non-diffracting beams with wave equation solutions in homogeneous media that are able to resist the effects of diffraction for long distances [32,42,43]. These beams all have a self-healing feature after scattering since they preserve the beam intensity profile after distortion [44,45]. The self-healing property has been demonstrated experimentally using scanned Bessel beams for microscopy through scattering materials, including glass beads and human skin, yielding reduced scattering artifacts, improved image quality, and increased penetration depth [46]. Another unique feature of these beams is that they all have an accelerating trajectory, i.e. a bending propagating trajectory as defined by the main peak location [43,47–49]. Within the non-diffracting beams family, Airy beams have been the focus of research for imaging since they have an almost three times larger penetration depth compared to Bessel beams [50]. The use of holography to modulate the spatial phase front, thereby converting Gaussian beams into Airy beams, has been widely studied. [51-54]. More interestingly, this approach can generate an array of Airy beams from one single-phase mask [55]. All these accelerating beams have side fringes in their beam intensity profiles, and, as mentioned above, two-photon excitation can reduce the noise produced by the side fringes. Therefore, integrating Airy beams into two-photon light-sheet microscopy will significantly increase the penetration depth and reduce the noise from side fringes. Until recently, only limited work has been focusing on this direction [56,57]. The focus of this study is to develop a two-photon flow cytometer with laser scanning 2D Airy beams as the light source. This scanned Airy beam forms a light-sheet that will fully cross-section microfluidic channels in the dimensions close to $100~\mu m$, demonstrating its potential for future study within live animals.

2. Methods

The schematic drawing of this setup is shown in Fig. 1. The light source is a femtosecond laser (100 fs, 690 nm to 1040 nm, 2.5 W, Mai Tai HP, Spectra-Physics). The laser beam is expanded through a telescope to match the size of the spatial light modulator (SLM, active area diagonal of 0.7" with an aspect ratio of 16:9, PLUTO-NIR-010, Holoeye Photonics). The phase profile for each Airy beam on the SLM is calculated and loaded onto the SLM via a personal computer. After leaving the SLM, the Airy beam passes through a pair of relay lenses to reduce its diameter to match the size of the galvanometric mirror, which scans the Airy beam in the horizontal direction to produce a light sheet. After passing through another pair of relay lenses, the scanned Airy beam is directed into an objective lens (Nikon Apo VC 60×1.20 WI). This light-sheet then cross sections the microfluidic channel (75 μ m \times 75 μ m, 02-0768-0106-05, Labsmith). The suspended microspheres in media flow through the microfluidic channel at speeds up to 2.0 mm/s (0.0012 ml/min). The flow speed is controlled by a syringe pump (Fusion 200, Chemyx). To achieve potential in vivo cell counting capability, it is necessary to implement epi-detection through the illumination objective; therefore, a dichroic mirror is used to reflect the fluorescence signal into a PMT (R10699, Hamamatsu) with bandpass filters. A data acquisition (DAQ) card (USB-6341-BNC, National Instruments) collects the electrical signal from the PMT. Data from the DAQ card is automatically captured via a Python script, and a separate Python script analyzes the number of fluorescent peaks to provide a count. Captured data is smoothed using a moving-window average of 10 consecutive sample points.

Fluorescent microspheres with an excitation peak at 505 nm and emission peak at 515 nm were purchased from Fisher Scientific (Invitrogen FluoSpheres Polystyrene Microspheres, 15 μ m diameter, yellowgreen fluorescent 505/515). The testing solution was prepared in a two-stage process by suspending the microspheres in a predetermined volume of polysorbate 80 (PS80) in a microcentrifuge tube that was first agitated with a vortex mixer to ensure proper solution and suspension before adding distilled water to bring the solution to a concentration of 2.0×10^5 spheres/mL and 1% PS80, by volume. Then it was

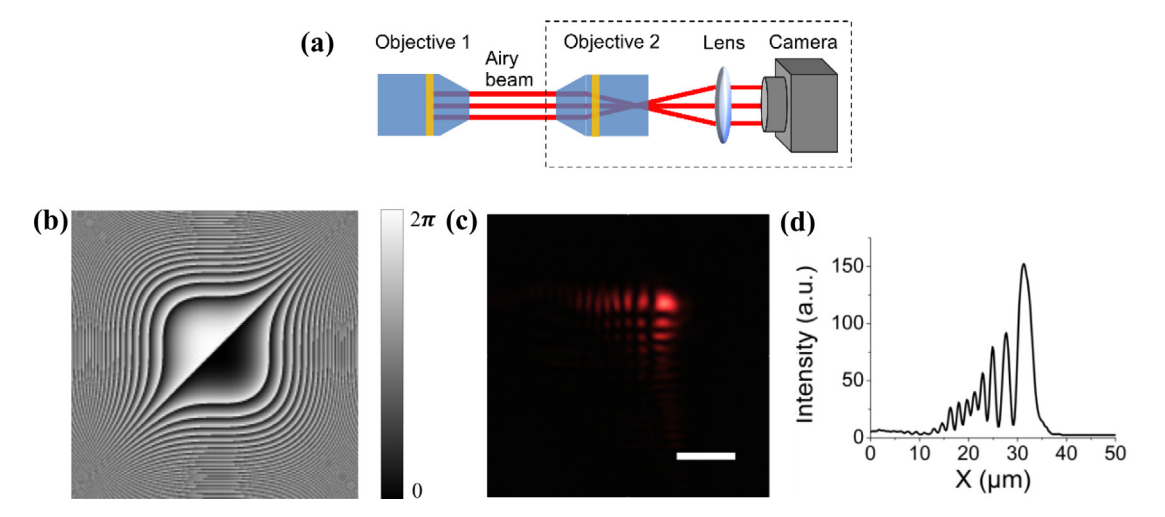


Fig. 2. 2D Airy beam characterization. (a) The telescopic setup (dashed box) to measure Airy beam profile includes a second objective, a lens, and a camera. (b) Phase mask displayed on SLM to generate 2D Airy beams. (c) Intensity of the 2D Airy beam recorded by a CCD camera. Scale bar: 10 μm. (d) Intensity profile across the 2D Airy beam in x-direction

agitated again in the vortex mixer before being placed into the syringe pump. This process allows the PS80 to coat the microspheres properly and prevents agglomeration for smooth flow within the syringe pump and microfluidic channels.

3. Results

The average speed of flowing cells in the human body is about 1 mm/s, and the diameter of these cells is about 10 μm . It takes about 10 ms for a single cell to pass through the cross-section of the blood vessel. To ensure that the scanned 2D Airy beam intersects each flowing cell at least once, the minimum scanning rate must be 100 Hz. In our experiment, this scanning rate was set at 444 kHz. Assuming the size of the blood vessel is 100 μm , the dwelling time of the Airy beam on the cell is about 0.09 ms. Therefore, the sampling rate of the DAQ card was set at 250 ks/s. Ideally the main lobe of the 2D Airy beam would occupy a high percentage of the total beam energy for efficient two-photon excitation. On the other hand, to maintain a long Rayleigh range, the Airy beam needs to have more side lobes, which takes up more energy. Therefore, there is a trade-off between these two requirements. The spatial Fourier spectrum of 1D Airy beam is given by the equation

$$\phi_0(k) = \exp(-ak^2) \exp(\frac{i}{2}(k^3 - 3a^2k - ia^3)),$$

where k is the normalized spatial frequency, and a is a decay factor determining Airy side lobes [58]. Propagation of Airy beams in free space and after focus has been studied before [59,60]. In this flow cytometer setup with a 60× objective, we are using a tightly focused Airy beam for detecting microscopic structures. The shorter the focal length of the objective lens is, the shorter the Rayleigh range is [59]. We varied the parameter a in a range to find the appropriate Rayleigh range $\sim 100 \ \mu m$ to fully intersect the vessel in the experiment.

In order to measure the beam profile of the Airy beams at the focus of the illumination objective lens, we constructed a telescope (Fig. 2(a), dashed box) to expand this Airy beam and project it onto a CMOS camera. One dimensional (1D) Airy beams have been commonly generated for characterization. However, they are not suitable for light-sheet microscopy since the non-diffracting behavior only happens in the Airy function dimension (x). In the other lateral dimension (y) the 1D Airy beam still has diffraction behavior. We have generated 2D Airy beams by using the appropriate phase mask, shown in Fig. 2(b). It is displayed on the SLM and fills up the center portion of the SLM, and the incident Gaussian beam size matches the size of this SLM. The phase modulation in each dimension (x and y) is a third order function of normalized lateral wave vectors (x and x) is a third order function of

are measured with the telescope setup in Fig. 2(a), and the results are shown in Fig. 2(c) and 2(d), which clearly demonstrate an Airy function. The FWHM of the main lobe in this Airy beam is about 3 µm. The main lobe contains about 70% of the total beam energy, similar to previous experiments [61]. The phase modulation depth determines the main lobe size, energy, and the number of side lobes. This will be discussed below.

We further characterized these 2D Airy beams' propagation in the z-direction. The intensity features of this exemplary Airy beam remained invariant up to 100 µm (Figs. 3(a)-3(e)). Although ideal Airy beams have infinitely long non-diffracting propagation distances, experimentally generated Airy beams are always truncated by factors such as objective lens aperture and hence can only achieve limited non-diffracting propagation distances. We were able to generate Airy beams with non-diffracting distances around 100 µm to form light-sheet cross-sections of a microchannel of similar size. Longer non-diffracting distance requires greater phase modulation depth, which leads to more side lobes, reduced main lobe energy, and lower two-photon excitation efficiency. Therefore, there is a trade-off while developing Airy beams for deep vessel cytometry and imaging. The accelerating behavior in two dimensions of this 2D Airy beam is clearly demonstrated in Fig. 3(f), where the main lobe's peak-intensity location is plotted vs. the propagation direction (z). The main lobe's parabolic trajectory becomes evident in both x and y directions. For clarification, this acceleration behavior only refers to the peak intensity of the main lobe, while the center of gravity of the wave front energy still propagates in a straight line. As mentioned above, the depth of phase modulation determines the Airy beam lobe features. We used an empirical parameter k_i to describe such phase modulation in each dimension (x & y), which is effectively a wave vector of the phase change patterns in real space. The higher this k_i is, the faster the phase change is, and consequently the more prominent the side lobes are. Fig. 3(g) compares the propagation phenomena of three Airy beams with $k_i = 5$, 6, and 7. The FWHMs in the z-direction of these three Airy beams are 80, 90, and 100 μm respectively for $k_i = 5$, 6, and 7, demonstrating that the propagation invariant distance increases as the phase modulation increases. We chose Airy beams with $k_i = 7$ for later flow cytometry experiments to ensure good intersection with the microfluidic channel of a cross-sectional area $75 \ \mu m \times 75 \ \mu m$.

Scanning this 2D Airy beam using a galvanometric mirror formed a light-sheet in the x–z plane (Fig. 3(h)). The span of this light-sheet in the x-direction was about 100 μ m, and the scan rate was 1 kHz. Considering that the flow speed within an artery is on the order of 1 mm/s, and that the diameter of microspheres/leukocytes is about

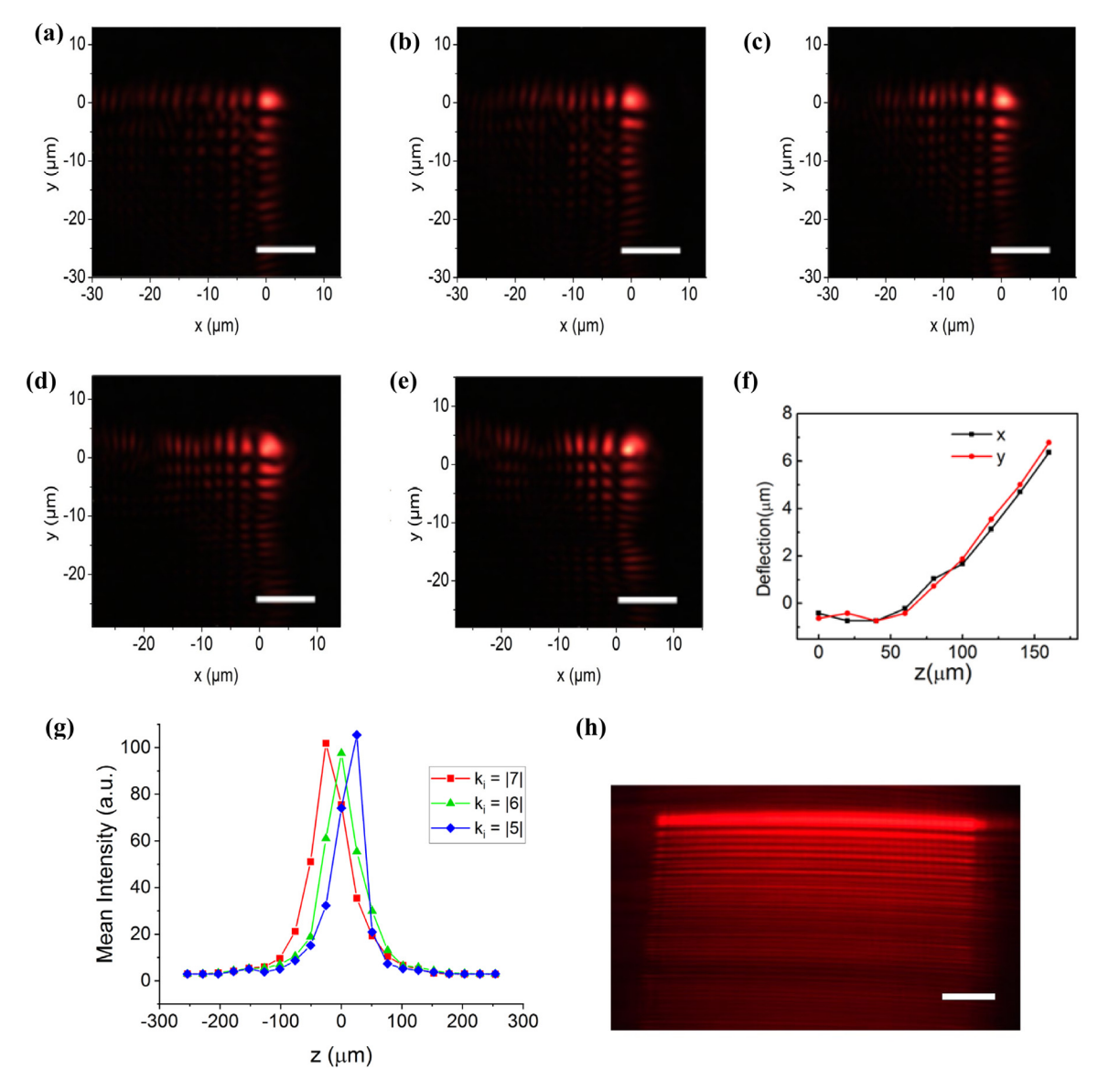


Fig. 3. Airy beam propagation. Intensity image of a 2D Airy beam at (a) z = 0 μm, (b) 25 μm, (c) 50 μm, (d) 75 μm, (e) 100 μm, and (f) the accelerating trajectory of this 2D Airy beam. (g) Peak intensity of Airy beams in the z-direction. Airy phase masks are defined by the parameter k_i , which determines the amount of phase modulation. Here we show three values, where $k_i = 5$, 6, and 7. (h) Cross-sectional view of the scanned 2D Airy beam in the x-z plane. Scale bar: 10 μm.

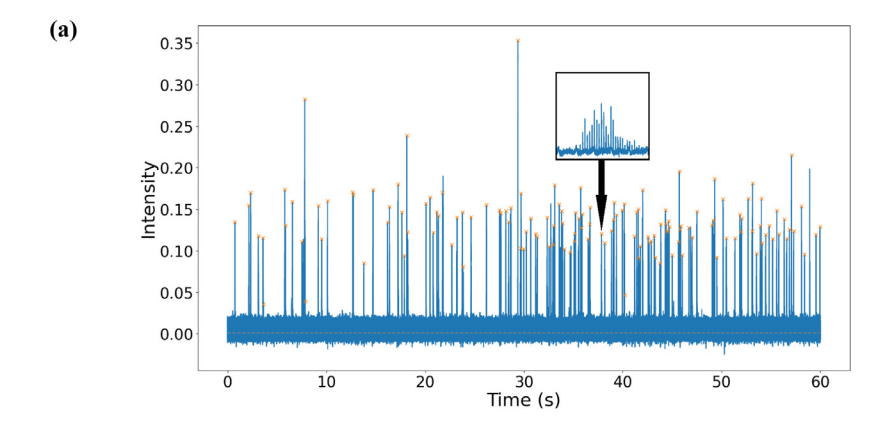
 $10~\mu m$, it would therefore take 10~ms for a single leukocyte to pass through this light-sheet. Therefore, we determined that a scan rate of 1~kHz would easily ensure multiple excitations of fluorescence from each flowing particle and result in repeated peaks in the time trace of recorded signals. There were multiple side light-sheets due to scanned side lobes. Since the main lobe contains the majority of the light energy ($\sim\!70\%$), two-photon excitation was predicted to significantly suppress the fluorescence signals generated by these side sheets.

Next, for the two-photon excitation of flowing fluorescent microspheres, we generated a light-sheet with 720 nm light at a scanning rate of 444 Hz. A microsphere solution, prepared as described above at 2.0×10^5 spheres/mL and 1% PS80, was placed in a syringe pump with a flow rate of 3.0×10^{-4} ml/min. The fluid velocity through this microfluidic channel was estimated to be about 0.9 mm/s with the intended rate of 1 sphere/s flowing through this light-sheet. The data acquisition rate of the DAQ card was 250,000 samples/s. We expected to see each microsphere emit fluorescent signal for about 1.60×10^{-2} seconds, corresponding to 7.4 scans of the galvanometric mirror per microsphere. A representative trace of the fluorescence signals is shown in Fig. 4(a). The signal-to-noise ratio was around 10, and each peak

comprised multiple peaks at a period of 1.1×10^{-3} seconds, as shown in the zoomed-in view (inset in Fig. 4(a) and Fig. 4(b)),. Since the scanning rate of this Airy beam was 444 Hz, the laser beam intersected the flowing microspheres at a rate of 888 Hz from the forward and backward scans. Hence, the theoretical period of fluorescence signals is about 1.1×10^{-3} seconds, which matches the experimental result. Analysis of these fluorescence signals found that microsphere velocities ranged from 0.3 mm/s to 0.9 mm/s. We recorded 10 one-minute traces (Supplementary Data) and calculated the average rate of detected peaks to be 75 peaks/min, which is close to the predicted frequency of 60 microspheres/min. Together with the SNR of 10, this light-sheet flow cytometer demonstrated a high detection rate of such flowing microspheres.

4. Summary

We have explored the feasibility of using scanning 2D Airy beams to form a light-sheet for two-photon flow cytometry. The non-diffracting distance of such beams ensures a large cross-sectional area with efficient two-photon excitation, which would enable the sampling of flowing cells in large-diameter arteries and veins. Our results demonstrate



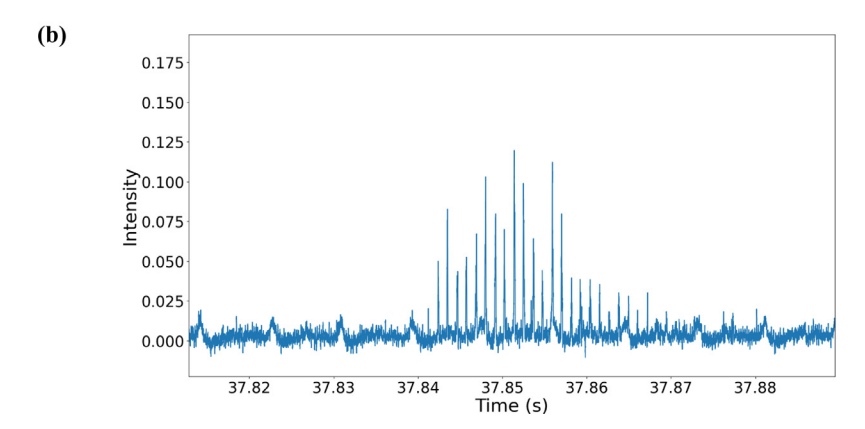


Fig. 4. (a) One representative trace of 15-µm fluorescent microspheres flowing through a microfluidic channel. (b) Enlarged view of one peak from (a).

the generation of such a light-sheet with over 100 μm non-diffracting distance. This light-sheet can efficiently detect fluorescent microspheres flowing at a speed of ${\sim}1$ mm/s in a microfluidic channel of a cross-sectional area 75 $\mu m \times 75$ μm at a signal-to-noise ratio of 10. Future directions include developing this modality for *in vivo* detection of flowing cells. Due to their self-healing properties, Airy beams are ideal candidates for such deep tissue applications.

CRediT authorship contribution statement

Aurelio Paez: Methodology, Writing – original draft, Software, Editing. **Emma M. Sundin:** Methodology, Writing – original draft, Editing. **Gilberto Navarro:** Methodology. **Xiujun Li:** Conceptualization, Funding acquisition. **Thomas Boland:** Conceptualization. **Chunqiang Li:** Conceptualization, Funding acquisition, Methodology, Supervision, Editing.

Declaration of competing interest

The authors declare that they have no known competing financial interests or personal relationships that could have appeared to influence the work reported in this paper.

Acknowledgment

US National Science Foundation (NSF) (1827745).

Appendix A. Supplementary data

Supplementary material related to this article can be found online at https://doi.org/10.1016/j.optcom.2021.127804.

References

- V.V. Tuchin, Advanced Optical Flow Cytometry: Methods and Disease Diagnoses, John Wiley & Sons, 2011.
- [2] J. Novak, I. Georgakoudi, X. Wei, A. Prossin, C.P. Lin, In vivo flow cytometer for real-time detection and quantification of circulating cells, Opt. Lett. 29 (2004) 77
- [3] V.V. Tuchin, A. Tárnok, V.P. Zharov, In vivo flow cytometry: A horizon of opportunities, Cytometry Part A 79A (2011) 737–745.
- [4] Z. Fan, X. Wei, In vivo flow cytometry: A powerful optical technology to detect circulating tumor cells and diagnose cancer metastasis in vivo, Photonics Lasers Med. 2 (2013) 27–35.
- [5] Y.J. Fan, et al., Microfluidic channel integrated with a lattice lightsheet microscopic system for continuous cell imaging, Lab Chip 21 (2021) 344–354.
- [6] D. Psaltis, S.R. Quake, C. Yang, Developing optofluidic technology through the fusion of microfluidics and optics, Nature 442 (2006) 381–386.
- [7] I. Georgakoudi, et al., In vivo flow cytometry: A new method for enumerating circulating cancer cells, Cancer Res. 64 (2004) 5044–5047.
- [8] D.A. Sipkins, et al., In vivo imaging of specialized bone marrow endothelial microdomains for tumour engraftment, Nature 435 (2005) 969–973.
- [9] W. He, H. Wang, L.C. Hartmann, J.-X. Cheng, P.S. Low, In vivo quantitation of rare circulating tumor cells by multiphoton intravital flow cytometry, Proc. Natl. Acad. Sci. 104 (2007) 11760–11765.
- [10] E.I. Galanzha, et al., In vivo magnetic enrichment and multiplex photoacoustic detection of circulating tumour cells, Nat. Nanotechnol. 4 (2009) 855–860.
- [11] E.I. Galanzha, E.V. Shashkov, P.M. Spring, J.Y. Suen, V.P. Zharov, In vivo, non-invasive, label-free detection and eradication of circulating metastatic melanoma cells using two-color photoacoustic flow cytometry with a diode laser, Cancer Res. 69 (2009) 7926–7934.
- [12] Z.C. Fan, et al., Real-time monitoring of rare circulating hepatocellular carcinoma cells in an orthotopic model by in vivo flow cytometry assesses resection on metastasis, Cancer Res. 72 (2012) 2683–2691.
- [13] K. Pang, et al., Monitoring circulating prostate cancer cells by in vivo flow cytometry assesses androgen deprivation therapy on metastasis, Cytom. Part A 93 (2018) 517–524.
- [14] T. Pons, et al., In vivo imaging of single tumor cells in fast-flowing bloodstream using near-infrared quantum dots and time-gated imaging, ACS Nano 13 (2019) 3125–3131.

- [15] X. Tan, et al., In vivo flow cytometry of extremely rare circulating cells, Sci. Rep. 9 (2019) 3366.
- [16] Y. Suo, Z. Gu, X. Wei, Advances of in vivo flow cytometry on cancer studies, Cytom. Part A 97 (2020) 15–23.
- [17] J. Nolan, et al., In vivo flow cytometry of circulating tumor-associated exosomes, Anal. Cell. Pathol. 2016 (2016).
- [18] Z. Fan, et al., In vivo tracking of 'color-coded' effector, natural and induced regulatory T cells in the allograft response, Nat. Med. 16 (2010) 718–722.
- [19] C. Cai, et al., In vivo photoacoustic flow cytometry for early malaria diagnosis, Cytom. Part A 89 (2016) 531–542.
- [20] C. Cai, et al., Photoacoustic flow cytometry for single sickle cell detection In Vitro and In Vivo, Anal. Cell. Pathol. 2016 (2016).
- [21] E.I. Galanzha, et al., In vivo flow cytometry of circulating clots using negative photothermal and photoacoustic contrasts, Cytom. Part A 79A (2011) 814–824.
- [22] M.V. Novoselova, et al., Optical clearing for photoacoustic lympho- and angiography beyond conventional depth limit in vivo, Photoacoustics 20 (2020) 100186
- [23] E.A. Genina, et al., Rapid ultrasound optical clearing of human light and dark skin, IEEE Trans. Med. Imaging 39 (2020).
- [24] N.G. Horton, et al., In vivo three-photon microscopy of subcortical structures within an intact mouse brain, Nat. Photon, 7 (2013) 205–209.
- [25] Chang Y.-C. others, Fiber-optic multiphoton flow cytometry in whole blood and in vivo, J. Biomed. Opt. 15 (2010) 047004.
- [26] E.R. Tkaczyk, A.H. Tkaczyk, Multiphoton flow cytometry strategies and applications, Cytometry Part A 79A (2011) 775–788.
- [27] L. Kong, J. Tang, M. Cui, Multicolor multiphoton in vivo imaging flow cytometry, Ont. Express 24 (2016) 6126–6135.
- [28] W. Steenbergen, V.P. Zharov, Towards reaching the total blood volume by in vivo flow cytometry and theranostics, Cytom. Part A 95 (2019) 1223–1225.
- [29] A.H. Voie, D.H. Burns, F.A. Spelman, Orthogonal-plane fluorescence optical sectioning: Three-dimensional imaging of macroscopic biological specimens, J. Microsc. 170 (1993) 229–236
- [30] T.V. Truong, W. Supatto, D.S. Koos, J.M. Choi, S.E. Fraser, Deep and fast live imaging with two-photon scanned light-sheet microscopy, Nature Methods 8 (2011) 757–762.
- [31] J. Durnin, J.J. Miceli, J.H. Eberly, Diffraction-free beams, Phys. Rev. Lett. 58 (1987) 1499–1501.
- [32] J. Durnin, Exact solutions for nondiffracting beams. I. The scalar theory, J. Opt. Soc. Amer. A 4 (1987) 651–654.
- [33] J. Durnin, J.J. Miceli, J.H. Eberly, Comparison of bessel and Gaussian beams, Opt. Lett. 13 (1988) 79–80.
- [34] T.A. Planchon, et al., Rapid three-dimensional isotropic imaging of living cells using bessel beam plane illumination, Nature Methods 8 (2011) 417–423.
- [35] F.O. Fahrbach, A. Rohrbach, Propagation stability of self-reconstructing bessel beams enables contrast-enhanced imaging in thick media, Nature Commun. 3 (2012) 1–8.
- [36] Zhang S. others, Scattering of a non-paraxial bessel light-sheet by a sphere of arbitrary size, J. Quant. Spectrosc. Radiat. Transfer 245 (2020) 106869.
- [37] F.O. Fahrbach, V. Gurchenkov, K. Alessandri, P. Nassoy, A. Rohrbach, Light-sheet microscopy in thick media using scanned bessel beams and two-photon fluorescence excitation, Opt. Express 21 (2013) 13824–13839.
- [38] B.C. Chen, et al., Lattice light-sheet microscopy: Imaging molecules to embryos at high spatiotemporal resolution, Science 346 (80) (2014).

- [39] G. Thériault, M. Cottet, A. Castonguay, N. McCarthy, Y. De Koninck, Extended two-photon microscopy in live samples with bessel beams: Steadier focus, faster volume scans, and simpler stereoscopic imaging, Front. Cell. Neurosci. 8 (2014) 139
- [40] M. Zhao, et al., Cellular imaging of deep organ using two-photon bessel lightsheet nonlinear structured illumination microscopy, Biomed. Opt. Express 5 (2014) 1296–1308.
- [41] B.B. Collier, S. Awasthi, D.K. Lieu, J.W. Chan, Non-linear optical flow cytometry using a scanned, bessel beam light-sheet, Sci. Rep. 5 (2015) 1–8.
- [42] H.E. Hernández-Figueroa, M. Zamboni-Rached, E. Recami, Non-Diffracting Waves, John Wiley & Sons, 2013.
- [43] I. Kaminer, R. Bekenstein, J. Nemirovsky, M. Segev, Nondiffracting accelerating wave packets of Maxwell's equations, Phys. Rev. Lett. 108 (2012) 163901.
- [44] J. Baumgartl, M. Mazilu, K. Dholakia, Optically mediated particle clearing using Airy wavepackets, Nat. Photon. 2 (2008) 675–678.
- [45] J. Broky, G.A. Siviloglou, A. Dogariu, D.N. Christodoulides, Self-healing properties of optical Airy beams, Opt. Express 16 (2008) 12880–12891.
- [46] F.O. Fahrbach, P. Simon, A. Rohrbach, Microscopy with self-reconstructing beams, Nat. Photon. 4 (2010) 780–785.
- [47] E. Greenfield, M. Segev, W. Walasik, O. Raz, Accelerating light beams along arbitrary convex trajectories, Phys. Rev. Lett. 106 (2011) 213902.
- [48] F. Courvoisier, et al., Sending femtosecond pulses in circles: highly nonparaxial accelerating beams, Opt. Lett. 37 (2012) 1736.
- [49] P. Zhang, et al., Generation of linear and nonlinear nonparaxial accelerating beams, Opt. Lett. 37 (2012) 2820.
- [50] T. Vettenburg, et al., Light-sheet microscopy using an Airy beam, Nature Methods 11 (2014) 541.
- [51] R.A.B. Suarez, T.A. Vieira, I.S.V. Yepes, M.R.R. Gesualdi, Photorefractive and computational holography in the experimental generation of Airy beams, Opt. Commun. 366 (2016) 291–300.
- [52] Q. Lu, S. Gao, L. Sheng, J. Wu, Y. Qiao, Generation of coherent and incoherent Airy beam arrays and experimental comparisons of their scintillation characteristics in atmospheric turbulence, Appl. Opt. 56 (2017) 3750–3757.
- [53] Y. Jiang, S. Zhao, W. Yu, X. Zhu, Abruptly autofocusing property of circular Airy vortex beams with different initial launch angles, J. Opt. Soc. Amer. A 35 (2018) 890–894.
- [54] I.S.V. Yepes, T.A. Vieira, R.A.B. Suarez, S.R.C. Fernandez, M.R.R. Gesualdi, Phase and intensity analysis of non-diffracting beams via digital holography, Opt. Commun. 437 (2019) 121–127.
- [55] R.A.B. Suarez, A.A.R. Neves, M.R.R. Gesualdi, Optical trapping with nondiffracting airy beams array using a holographic optical tweezers, Opt. Laser Technol. 135 (2021) 106678.
- [56] P. Piksarv, et al., Integrated single- and two-photon light sheet microscopy using accelerating beams, Sci. Rep. 7 (2017) 1435.
- [57] N.A. Hosny, et al., Planar Airy beam light-sheet for two-photon microscopy, Biomed. Opt. Express 11 (2020) 3927.
- [58] G.A. Siviloglou, D.N. Christodoulides, Accelerating finite energy Airy beams, Opt. Lett. 32 (2007) 979–981.
- [59] R.A.B. Suarez, M.R.R. Gesualdi, Propagation of airy beams with ballistic trajectory passing through the Fourier transformation system, Optik (Stuttg). 207 (2020) 163764
- [60] K. Cheng, X. Zhong, A. Xiang, Propagation dynamics and optical trapping of a radial airy array beam, Optik (Stuttg) 125 (2014) 3966–3971.
- [61] G.A. Siviloglou, J. Broky, A. Dogariu, D.N. Christodoulides, Observation of accelerating Airy beams, Phys. Rev. Lett. 99 (2007) 213901.